A Flexible Dielectric Scattering Surface Realized with Graphite Doped Silicone

Mehmet Emre Eralp*,‡, Isin Ozgen†, Burak Ferhat Ozcan†, Sema Dumanli†, Ozlem Aydin Civi*
*Middle East Technical University, Ankara, Turkiye, ozlem@metu.edu.tr
†Bogazici University, Istanbul, Turkiye, sema.dumanli@bogazici.edu.tr
‡Accelerate Simulation Technologies, Ankara, Turkiye

***Abstract*—This paper presents a flexible and low-profile dielectric scattering surface designed for RCS reduction without using metallic patterns. The surface is fabricated from graphite-doped silicone, which allows for dielectric constant control between 3 and 15. The surface maintains a constant thickness of 2.5 mm, while the reflection phase of the dielectric cells is controlled by varying the dielectric constant. Two phase distributions are investigated: a checkerboard configuration for monostatic RCS reduction, and a modified cubic phase distribution for enhanced bistatic RCS reduction. Simulation results show that the proposed flexible checkerboard achieves a 10 dB monostatic reduction while the modified cubic phase distribution effectively suppresses bistatic reflections more than 14 dB at all angles. The proposed design offers a lightweight and conformal solution for electromagnetic stealth applications in X band.**

***Index Terms*—Dielectric surfaces, scattering surfaces, RCS reduction, graphite-doped silicone, phase distribution.**

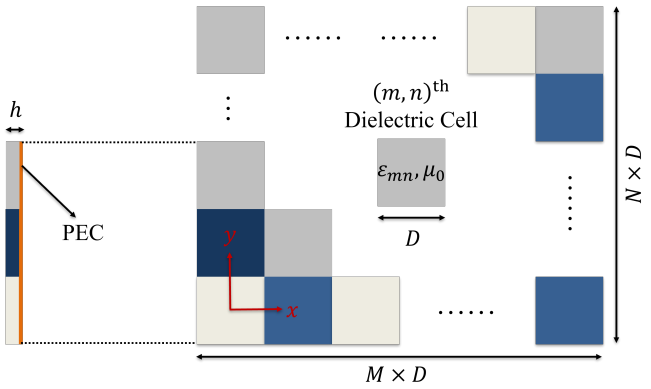

Fig. 1. Side and top view of the dielectric scattering surface.

I. Introduction

Radar Cross Section (RCS) reduction techniques have attracted significant attention for the electromagnetic stealth of various platforms in defense and security. Extensive research has been conducted on metamaterial-based surfaces, which often rely on metallic patterns and suffer from heavier and more complex structures or mechanical rigidity [1], [2], [3]. In recent years, dielectric surfaces have emerged as an effective alternative for low-profile RCS reduction, utilizing reflection phase distributions on the surface to redirect the backscattered waves away from the incident direction [4], [5].

Previously, a 3D-printed dielectric scatterer based on thermoplastic materials, such as polylactic acid (PLA), has been reported to achieve monostatic RCS reduction [6]. However, this design is inherently rigid and lacks the mechanical flexibility required for conformal applications. Furthermore, phase control in such a design typically depends on both dielectric constant and thickness variation. Because the range of dielectric constants that can be achieved with this approach is limited, the design needs to have an intended shape, which limits structural uniformity.

In this study, we propose a new approach in RCS reduction that employs graphite doped silicone as the constitutive material for a dielectric scattering surface. The use of silicone provides mechanical flexibility, while the inclusion of graphite powder can be used to tune electromagnetic properties by adjusting the filler ratio. The proposed design maintains a constant thickness and achieves the desired phase variation solely through the material's dielectric constant. Measured results from fabricated samples show that the dielectric constant can be varied from 3 to 15, offering a wide design range for the reflection phase distribution.

Beyond the classical checkerboard phase distribution, which mainly reduces monostatic reflections, a cubic phase distribution is used to achieve diffuse reflection and reduce bistatic reflection. The overall objective is to realize a low-profile, mechanically flexible, and thin dielectric surface that performs effectively across X band and can conform to various platform geometries with curved surfaces.

II. Design Procedure

A. Phase Characteristics

RCS reduction in scattering surfaces is achieved by making the reflected fields interfere destructively. This is typically accomplished by creating a phase distribution on the surface such that the reflected fields cancel each other in the far zone. The surface is divided into a number of cells or regions, where the reflection phase is assumed to be constant. The geometry of the dielectric scattering surface used in this study is shown in Fig. 1. Each cell is modeled as a grounded dielectric slab of thickness h and side length D, with varying dielectric constant $\varepsilon_{r,mn}$. When a plane wave is normally incident on such a slab backed by a perfect conductor, assuming it to be non-magnetic and lossless, the phase of the surface reflection coefficient of $(m,n)^{th}$ dielectric cell is determined by [4]

$$\psi_{mn} = 2\arctan(\sqrt{\varepsilon_{r,mn}}\cot(k_0 h\sqrt{\varepsilon_{r,mn}})), \qquad (1)$$

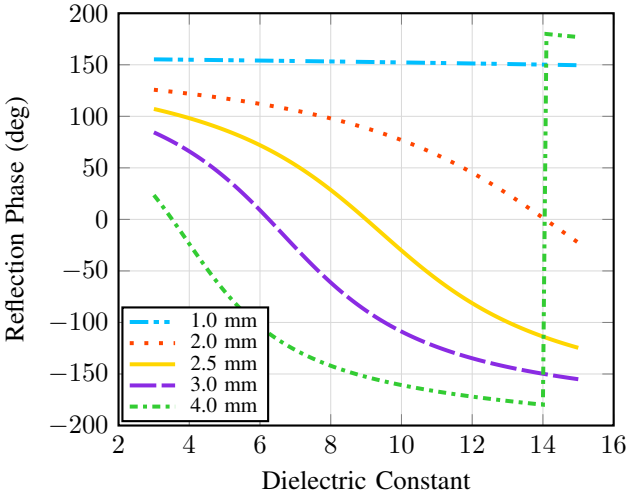

Fig. 2. Reflection phase as a function of dielectric constant for different substrate thicknesses at 10 GHz. The range of dielectric constant (3–15) corresponds to the measured values of the fabricated graphite doped silicone samples.

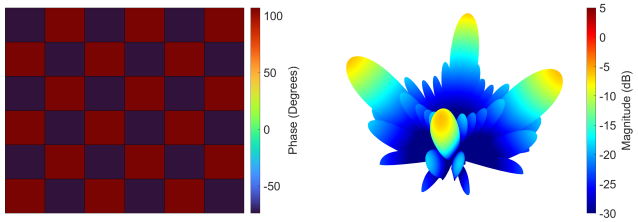

(a) (b)

Fig. 3. (a) Checkerboard phase distribution, (b) computed reflected field pattern at 10 GHz.

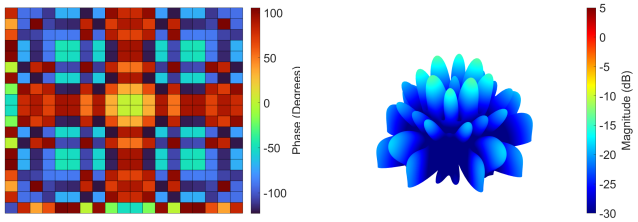

(a) (b)

Fig. 4. (a) Modified cubic phase distribution, (b) computed reflected field pattern at 10 GHz.

where k_0 is the free space propagation constant. The variation of the reflection phase at 10 GHz with respect to the dielectric constant for several constant thickness values is shown in Fig. 2. For thinner substrates, the phase variation is limited whereas thicker substrates provide a broader phase range. In this study, the dielectric constant range between 3 and 15 is considered according to the measured values of fabricated silicone–graphite samples. Details of the material preparation and dielectric characterization are provided in Section III. Based on these results, a substrate thickness of 2.5 mm is selected since it provides a more linear phase curve around $0°$ within the dielectric constant range of interest at 10 GHz.

B. Phase Distributions and Reflected Field Patterns

After obtaining the reflection phase characteristics, the reflected field patterns of checkerboard and cubic phase distributions are computed in MATLAB by implementing 2D planar array factor formulation. Each dielectric cell is modeled as an individual radiating element with a uniform amplitude and a reflection phase determined by (1). By superposing the contributions of all cells, the far field scattering pattern of the entire surface is predicted efficiently, allowing fast evaluation of different phase distributions before full wave simulations.

The checkerboard distribution is a well-known configuration for monostatic RCS reduction. It consists of two alternating dielectric cells with a reflection phase difference of approximately $180°$, resulting in destructive interference of the backscattered fields in the monostatic direction. In this design, a constant substrate thickness of $h = 2.5$ mm is used, and two dielectric constants are selected according to the reflection-phase curve presented in Fig. 2. The first dielectric constant, $\varepsilon_{r,11} = 3$, provides a reflection phase of $\psi_{11} = 107.15°$, whereas the second, $\varepsilon_{r,12} = 11.5$, yields a reflection phase of $\psi_{12} = -70.32°$. This shows that the required $180°$ phase difference can be achieved directly with practically realizable materials.

Each dielectric cell has a side length of $D = 30$ mm, determined according to the design approach reported in [6]. The total surface consists of 6×6 cells, forming a 180 *mm* $\times$ 180 *mm* surface. The checkerboard layout alternates the two dielectric materials along both the $x-$ and $y-$directions. Fig. 3 presents the designed checkerboard phase distribution and the computed reflected field pattern at 10 GHz.

To mitigate the strong bistatic lobes observed in checkerboard configuration, a cubic phase distribution can be used [3]. The reflection phase assigned to each dielectric cell (m, n) follows a symmetric cubic equation given by

$$\psi_{mn} = \frac{\alpha}{(ND)^3}\left(|x_m|^3 + |y_n|^3\right), \tag{2}$$

where α is the cubic alpha constant effective on reflected field pattern, and x_m, y_n denote the center coordinates of each cell along the $x-$ and $y-$axis, respectively. N is the number of dielectric cells along $y-$axis and taken as $N = M$. This formulation generates a symmetric and non-periodic phase variation, which redistributes the reflected fields into multiple angular directions. Thus, an improved bistatic reflection reduction performance can be obtained.

The phase values computed by (2) range from $-180°$ and $180°$ in principle interval. However, for the proposed design, the achievable reflection phase range is limited by the material characteristics and substrate thickness to approximately $-127°$ and $107°$ for $h = 2.5$ mm at 10 GHz, as shown in Fig. 2. Therefore, all the phase values outside this interval are scaled

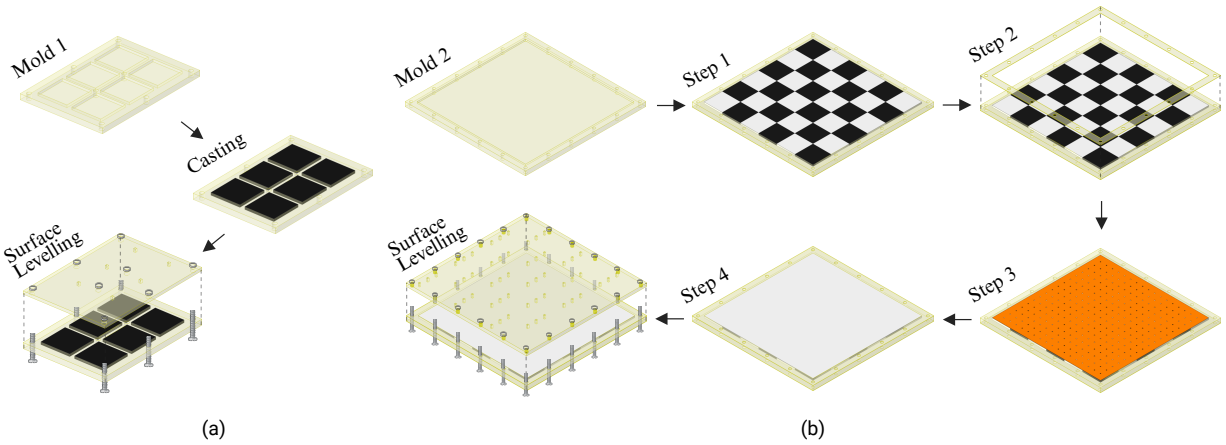

Fig. 5. Fabrication process of the proposed scattering surface designs.

into the attainable range, ensuring that each cell corresponds to dielectric constant within the measured interval of 3–15.

Using this modified phase profile, 20 × 20 cell surface is designed with $D = 10$ mm, resulting in a total surface of 200 mm × 200 mm. After observing the reflection patterns for several of them, one alternative α is chosen as 1340. The resulting phase distribution and its computed reflected field pattern at 10 GHz are shown in Fig. 4. This cubic design produces a significantly more diffuse scattering pattern compared to the checkerboard case, reducing both the monostatic and bistatic reflections with more than 14 dB in all directions.

III. Material Preparation and Fabrication

Silicone has been doped in the literature for various applications that require the tuning of the dielectric constant [7]. Graphite powder is among various dopants that can be utilized. We can develop flexible substrates with a dielectric constant of up to 15 by doping RTV-2 silicone with graphite powder. For this case, two types of substrates are required with target dielectric constants of 3 and 11.5. Undoped silicone can be used for the first target dielectric constant. For the second target dielectric constant, the silicone substrate is doped with graphite powder with a weight ratio of 4:10. Firstly, RTV-2 silicone is mixed with the graphite powder for at least 5 minutes. Subsequently, the curing agent is added to the mixture in a weight ratio of 1.8 % relative to the silicone base and mixed for 5 minutes. The final mixture is transferred to a 3D-printed mold including six 3 cm by 3 cm pools as seen in Fig 5(a). The substrates are degassed in a vacuum oven until all the air bubbles are removed. 3D printed leveling cover is screwed to the mold and the substrates are left for curing at room temperature for 8-10 hours. The undoped substrates are also produced in a similar manner.

Dielectric characterization of the samples is done with a DAK3.5-TL2 dielectric assessment kit [8]. All measurements are taken at the minimum applicable force of 20 N. The measurements are taken from five different points on the bottom and top surface of the samples. The dielectric constant values from 8 GHz to 12 GHz are given in Fig. 6, where solid lines represent the mean values and the shaded regions represent the variation. Mean dielectric constant values of 3.0 and 11.2 are achieved at 10 GHz.

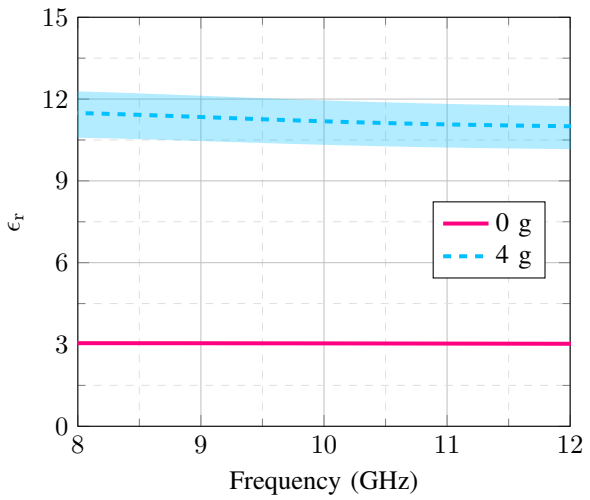

Fig. 6. Mean dielectric constant (ϵ_r) of silicone with 4 g graphite doping and without graphite.

As shown in Fig. 5(b), 18 doped and 18 undoped blocks are assembled in Mold 2 in a 6 × 6 checkerboard layout. Aquarium silicone is used to bond the substrates. In step 2, an alignment mold is placed on top of Mold 1. Then, the ground plane is positioned on top of the checkerboard layer. An undoped silicone layer with a thickness of 0.5 mm is then cast on top of the ground plane to encapsulate it, as shown in Step 4. The ground plane contains 1.5 mm diameter holes spaced 1 cm apart, which enhances adhesion between the silicone layers and improves the mechanical stability of the structure. The fabricated scattering surface is shown in Fig. 7.

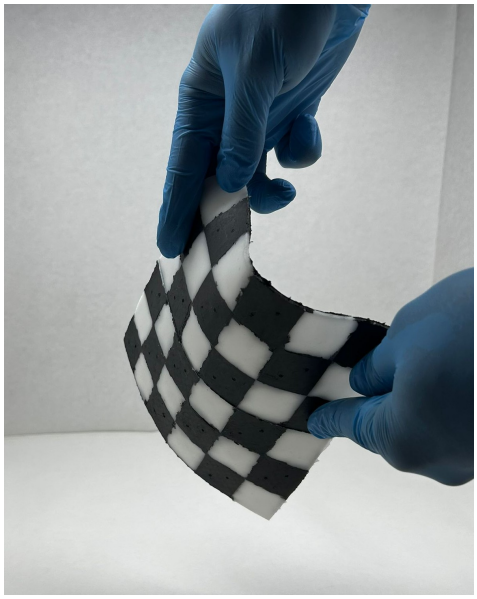

Fig. 7. Fabricated scattering surface.

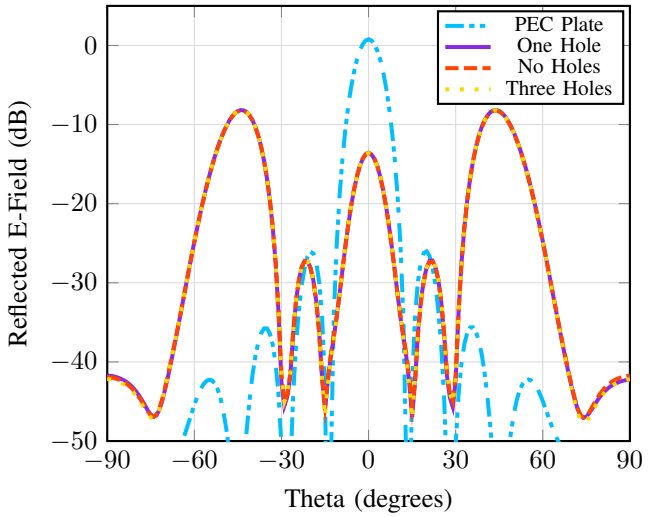

Fig. 8. Full-wave simulation results: Reflected E-field patterns on $\phi = 45°$ at 10 GHz.

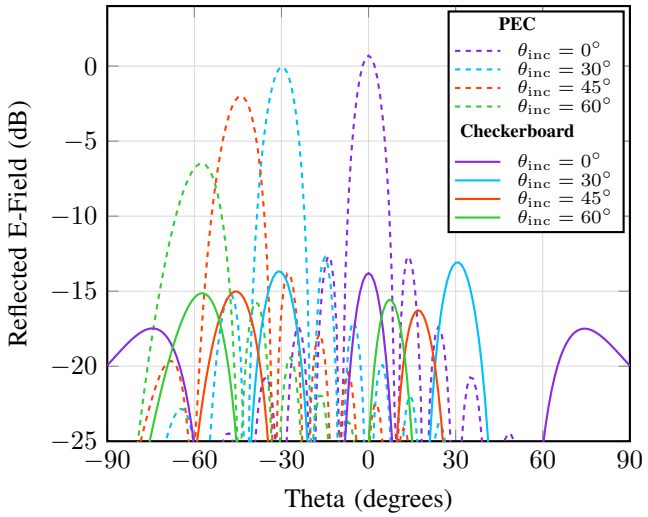

Fig. 9. Reflected E-field patterns on XZ plane at 10 GHz when the checkerboard is illuminated from different angles θ_{inc}.

IV. Simulation Results

Full wave electromagnetic simulations using HFSS are performed to evaluate the reflection reduction performance of the fabricated checkerboard surface. The simulations are carried out at 10 GHz under both normal and oblique incidences. The model includes the graphite doped dielectric cells and the metallic ground plane, which has small circular holes used in fabrication to improve mechanical bonding between the silicone and the ground. The results are compared against a reference PEC plate of the same size.

For the checkerboard design, Fig. 8 illustrates the simulated reflected E-field magnitude on the $\phi = 45°$ plane for normal incidence. The surface exhibits more than 10 dB backscattering reduction compared with the PEC reference. The effect of mechanical holes in the ground plane is also investigated. Three cases are considered: no holes, one hole, and three holes in a single dielectric cell. The presence of holes has almost no effect on the reflection pattern, which does not change the RCS reduction performance.

The angular stability of the checkerboard surface is examined for oblique incidences at $\theta_{inc} = 30°, 45°, 60°$. The corresponding reflected E-field patterns on the XZ-plane are presented in Fig. 9. Up to $\theta_{inc} = 60°$, the checkerboard surface effectively reduces the specular reflection by more than 10 dB, compared to the PEC plate. For $\theta_{inc} = 60°$, the reflection reduction can be seen as reasonable with a reduction of 8 dB. RCS reduction across a wide angular range demonstrates the angular robustness of the proposed dielectric design.

V. Conclusion

A flexible dielectric scattering surface based on graphite-doped silicone has been designed and analyzed for RCS reduction without using metallic patterns. The surface performs solely through variation in the dielectric constants of the cells while maintaining a constant thickness of 2.5 mm. Two dielectric cells with measured dielectric constants of 3.03 and 11.67 are used to realize a checkerboard configuration. Full wave simulation results confirm that the proposed checkerboard surface effectively suppresses monostatic reflections by more than 10 dB and remains robust under oblique incidence. In addition, a modified cubic phase distribution is investigated as an alternative, which is promising for bistatic reflection reduction as the analysis predicts more than 14 dB in all angular directions.

Future work will include reflection reduction measurements of the fabricated checkerboard surface to experimentally validate the simulation results. A flexible surface based on the modified cubic phase distribution will also be fabricated and measured. Furthermore, both designs will be simulated and

experimentally characterized on a cylindrical curved surface to evaluate their conformal performance. The RCS reduction bandwidth of the structures will be investigated, and sensitivity analyses will be conducted to assess the fabrication defects. The results of these configurations will be presented at the conference.

REFERENCES

[1] W. Chen, C. A. Balanis, and C. R. Birtcher, "Checkerboard EBG surfaces for Wideband radar cross section reduction," *IEEE Trans. Antennas Propag.*, vol. 63, no. 6, pp. 2636–2645, June 2015.

[2] M. F. El-Sewedy and M. A. Abdalla, "A monostatic and bistatic RCS reduction using artificial magnetic conductor metasurface," *IEEE Trans. Antennas Propag.*, vol. 71, no. 2, pp. 1988–1992, Feb. 2023.

[3] M. K. T. Al-Nuaimi, S. -L. Zhu, W. G. Whittow, G. -L. Huang, R. -S. Chen and Q. Shao, "Design of polarization-insensitive and angularly stable metasurfaces with symmetric cubic phase distribution for broadband RCS reduction," *IEEE Trans. Antennas Propag.*, vol. 72, no. 1, pp. 1069-1074, Jan. 2024.

[4] S. Qiu, Q. Guo, J. Su, and Z. Li, "Design of a dielectric dartboard surface for RCS reduction," *IEEE Antennas Wireless Propag. Lett.*, vol. 21, no. 2, pp. 401–405, Feb. 2022.

[5] Y. Saifullah, A. B. Waqas, G. M. Yang, and F. Xu, "Multi-bit dielectric coding metasurface for EM wave manipulation and anomalous reflection," *Opt. Exp.*, vol. 28, no. 2, pp. 1139-–1149. 2020.

[6] M. E. Eralp, Ö. Eris and Ö. A. Civi, "Analysis and design of fully dielectric scattering surface with additive manufacturing," in *Proc. 19th Eur. Conf. Antennas Propag.*, Stockholm, Sweden, 2025, pp. 1-3.

[7] J. Garrett, E. Fear, "Stable and flexible materials to mimic the dielectric properties of human soft tissues," in *IEEE Antennas and Wireless Propagation Letters*, vol. 13, pp. 599-602, 2014.

[8] Dak-TL2 for fast and precise dielectric measurement of thin layers, SPEAG, Schmid & Partner Engineering AG, https://speag.swiss/products/dak/for-dielectric-measurement-of-thin-layers-and-liquids-dak-tl2/.